



# Numerical and Experimental Study of the Stern Wedge Effects on the Hydrodynamics Performance of a Semi-Displacement Catamaran in Calm Water

M. Yousefifard<sup>†</sup> and A. Maboodi

Babol Noshirvani University of Technology, Babol, Iran

<sup>†</sup>Corresponding Author Email: [yousefifard@nit.ac.ir](mailto:yousefifard@nit.ac.ir)

(Received January 18, 2020; accepted August 27, 2020)

## ABSTRACT

In this article, the calm water resistance and dynamic instabilities of a semi-displacement catamaran fitted with a stern wedge is investigated using an experimental method and numerical technique. This is accomplished in order to probe into the effects of aft geometry modification on semi-displacement ship dynamic characteristics, especially at medium and high speeds. An advanced 6-DOF model that takes into consideration the dynamic mesh method has been utilized in open source code OpenFOAM. Reynolds-Average Navier-Stokes (RANS) equations are solved using standard  $k-\epsilon$  turbulence model and VOF method. The accuracy of the current numerical method is investigated by the calm water test in National Persian Gulf Towing Tank. The resistance, trim and sinkage of the ship were monitored during the experiments. The experimental analysis was performed on the initial model and a modified model with 8° wedge at different Froude numbers. After that, the wedges were mounted at different angles at the transom of the vessel and the effect of the angle change for 4 different angles was evaluated using numerical solution. The results show that fitting a stern wedge to this type of ship causes an intense pressure at the stern bottom. Also, it decreases the dynamic trimming and forward resistance of the craft. As well as, stern wedge causes increasing the lift force which affects the reduction of dynamic instabilities. It is concluded that numerical model presented here is quite suitable for accurately predicting dynamic characteristics of a semi-planing twin-hull ships at medium and high Froude numbers. As a result, 14% reduction in total resistance was observed due to the installation of a 6 degree stern wedge.

**Keywords:** Stern wedge; Catamaran; Dynamic instability; Experimental method; CFD.

## NOMENCLATURE

$C_t$	total resistance coefficient	ww	with-wedge
$f$	force	wow	without-wedge
$m$	mass of the ship	$X$	position vector
$M$	tensor of moments of inertia		
$n$	moment	$\alpha$	indicator function
$U$	velocity vector	$\rho$	density
$V_0$	ship or model speed	$\sigma$	surface tension
$p^*$	pseudo-dynamic pressure	$\mu_{eff}$	efficient dynamic viscosity
$g$	acceleration of gravity	$\mu_{urb}$	turbulent kinetic viscosity
$S$	wetted surface area	$\omega$	angular velocity

## 1. INTRODUCTION

The resistance of the planing vessel is heavily dependent on dynamic trim and rise-up as well

as sinkage. Creating lift force is the most important factor affecting the improvement of the performance and resistance of a high-speed crafts. Different appendages have been

developed over the years to reduce the drag force by creating a lift component. These appendages also have been proposed to improve the dynamic instabilities of planing and semi-planing hulls in calm water at high speeds. Stern wedge, trim tab, stern flap and interceptor are the most widely used appendages, utilized to improve the dynamic instabilities of high-speed craft. The stern wedge is a simple solid body with a triangular cross-section attached to the bottom of stern which reduces the trim by increasing the pressure normal to the hull surface near the stern region. The main focus of the researchers has been on the use of the desired equipment on high-speed craft. Because these devices have the most effect at very high speeds. As a result, little research has been done on the field of semi-displacement vessels. For this reason, in this study, the performance of one of these devices, which can be easily mounted on the hull, has been evaluated on the hydrodynamic performance of a semi-displacement vessel. Another difference of this research from the existing research in this field is the analysis of a twin-hull vessel by wedge installation. While, most existing researches are focused on mono-hull high-speed craft.

Next, the results of using each of these devices are reviewed by different researchers and their advantages and disadvantages are presented.

There have been many researches on numerical modeling and experimental investigation of instability control of high-speed crafts that have focused on fitting an appendage to create lift component and reduce dynamic trimming of the hull. Karafiath and Fisher (1987) presented one of the first investigations into the effect of stern wedge on hydrodynamic performance of a ship. They used a combination of model experiments and analytical method to evaluate the effect of stern wedge on the powering performance and annual fuel consumption of destroyer and frigate size ships. They used this method to minimize the powering penalty due to a wedge and decreased delivered power by 6 percent at maximum speed. Another early research in this area has been carried out by Jensen and Latorre (1992). They presented a description of a program called WEDGE that calculated the influence on the planing hull drag from fitting wedges or trim tabs. The presented results were compared with published examples and good results were obtained. Bojovic *et al.* (2004) have also done some research on the effect of using wedge on displacement vessels. They performed experimental study to present the results of the calm water test of a high-speed displacement hull forms with different combinations of spray rails with stern wedges. Considerable performance improvement has been reported in that research and the residuary resistance reduction in excess of 10% has been recorded

at higher speeds. Jadmiko *et al.* (2018) also used a CFD code to investigate the effect of stern wedge and stern flap on ship resistance reduction. They claimed that the use of stern wedge at low speeds could not improve the hydrodynamic performance of the vessel. Based on their result of simulations, the most optimal stern form performance reduces the resistance is stern flap 1% LPP with angle 4°. In this case, the resistance value was reduced 3.5% at 28 knots. It should be noted that, the results presented by the researchers show that in each case, the use of specific equipment has the advantage. Using the flap, Jadmiko *et al.* achieved a slight improvement in the hydrodynamic performance of the vessel.

Cumming *et al.* (2006) applied a stern flap and stern wedge installed on a fast planing boat to large surface ships. Their results showed that stern flap installation could not only reduce the ship resistance at the optimum speed by 9%, but also reduce the ship resistance in the cruise state. Jang *et al.* (2009) also studied the effects of appendages such as brackets and wedges on a high-speed passenger ferry, numerically.

Experimental studies were carried out by John *et al.* (2011) on a variety of hull models fitted with stern wedge, stern flap and interceptors. They performed model tests on fast displacement hull forms, planing crafts and foil assisted catamarans to study the effects of these devices on hydrodynamic performance. Based on their research, combined use of systems such as the stern wedge or the interceptor can be more effective in improving the hydrodynamic performance of the ship. However, proper justification for the use of any system depends on the type of ship and its speed. Recently, effects of a wedge on the performance of planing craft in calm water have been experimentally studied by Ghadimi *et al.* (2019). They combined the experimental measurements and theoretical 2D+T theory to bring deeper insight about physics of the flow and pressure distribution when a wedge was fitted. In their study, two different wedges with different angles have been added to the bare hull and their effects on the hydrodynamic performance of the planing craft have been evaluated. In both cases, a positive result is obtained from the installation of the wedge. Following this study, experimental and numerical investigation of stability and rooster tail of a mono-hull high-speed planing craft has been presented by Sajedi *et al.* (2019). They examined the effects of wedge dimensions on the reduction of resistance as well as generated wake profile dimensions behind the craft.

In the following, the results of research on other similar equipment will be presented. Day and Cooper (2011) experimentally investigated the impact of interceptors on the performance of a yacht hull. Their results showed a marked reduction in calm-water resistance over a wide

speed range, with benefits of 10-18% in the speed range between 8 and 20 knots. Karimi *et al.* (2013) carried out an experimental investigation on the effects of interceptor on hydrodynamic performance of high-speed planing crafts. Their results indicated a remarkable drag reduction of up to 15% for mono-hull model and up to 12% for catamaran model over the wide speed range of the models. According to their findings, the effect of installing the interceptor on low Froude numbers is completely reversed. As at Froude numbers less than 1.5, the increase in drag force is observed when the interceptor is installed. Salas and Tampier (2013) reported experimental and numerical results of the effects of appendages on forward resistance reduction of displacement and semi-displacement hull. The appendages evaluated in their study are stern flaps and interceptors for displacement hulls and spray rails for a semi-planing hull. The prediction of reduction in resistance is obtained around 5-10%. Mansoori and Fernandes (2015) presented hydrodynamic effects of interceptors on a 2-D flat plate based on both CFD and experimental approaches. They used Reynolds average Navier-Stokes (RANS) equation to model the flow around a fixed flat plate with an interceptor at different heights and attack angles. They also performed a numerical study on the effects of hydrodynamic interceptors on the propoising control (Mansoori and Fernandes, 2016). Using CFD method, they computed the pressure distribution created by interceptor and its effects on propoising. Based on their results, the interceptor can completely control the propoising phenomenon. They asserted that optimum choice of interceptor height had a great effect on its efficiency, and in choosing it the flow speed and length of the boat must be taken into consideration. Effect of main geometrical parameters of interceptors on hydrodynamic characteristics of a high-speed craft was investigated numerically by Mansoori *et al.* (2017). They stated that, the interceptor height should not be higher than 60 percent of boundary layer thickness at transom. Therefore, a system for controlling its height should be considered.

As well as, a study of the hydrodynamic performance of a deep-Vee ship was performed by Song *et al.* (2018) to determine the influence of the use of stern flaps and interceptors on drag-resistance, trim and sinkage properties of the ship. Their analysis results demonstrated that both the stern flap and interceptor resulting in reduce the amount of drag resistance, dynamic trimming and sinkage of the ship. The drag reduction rate attained in their study was of the order of 3-9%. Jangam *et al.* (2019) presented a CFD study to predict the pressure and resistance characteristics of a high-speed planing craft equipped with an interceptor and compared the numerical results with the experimental studies.

More experimental and numerical investigations have recently been made on the interceptor and its effect on the reduction of high-speed craft resistance. Park *et al.* (2019) developed experimentally an active control system using an interceptor to improve seakeeping performance of a high-speed planing vessel. Based on their research, an improvement in the resistance has been recorded at high Froude numbers and the pitch motion was decreased significantly in the regular and irregular waves by the controllable interceptor system. Avci and Barlas (2019) experimentally studied the effects of interceptor geometry on a planing-hull hydrodynamics. They suggested that the blades should be controlled separately at least in three parts from keel to chine area, if operable. According to their results, the length and location of the interceptor has a great effect on its hydrodynamic performance. Also, to achieve the best hydrodynamic performance, an intelligent system is needed to permanently control the interceptor. Song *et al.* (2019) illustrate the effect of interceptor installation on waterjet-ship wake fields. For this purpose, inlet velocity distribution of a semi-planing waterjet-propelled ship has been assessed via stereo particle image velocimetry (SPIV) measurements and Reynolds-averaged Navier-Stokes (RANS) simulations. Their results showed that in addition to decreasing the resistance, the installation of the interceptor had a good effect on the performance of the waterjet drive system.

It can be summarized that all dynamic instability control systems offer the most capability under certain conditions. The best choice depends on the type of vessel, its speed and hull form. Since the twin-hull ship presented in this research is a semi-displacement vessel, after observing the dynamic instability at design speed, it has been attempted to remove it with the least change in hull form as well as low cost. For this reason, the stern wedge was selected and its effects were evaluated numerically and experimentally.

In the current study, dynamic characteristics of semi-displacement catamaran are studied under Froude number up to 0.747 by OpenFOAM freeware. interDyMFoam solver has been used to considered 6-DOF motions of ship, and moving mesh model and VOF method has been implemented into to achieve more accurate results at high Froude numbers. A Finite Volume Method (FVM) has been employed accurately simulate complicate geometry and free surface. Forward resistance, dynamic trimming and model sinkage have been computed and compared against experimental measurements.

The most important goal of this research is to achieve a simple and effective way to reduce the required power of a semi-displacement

vessel at design speed. The design speed of the ship is determined in the initial design phase and the main dimensions and hull form of this vessel are designed accordingly. In fact, this speed is a function of the ship's performance criteria, such as carrying cargo on time. The hydrodynamic performance of a ship is evaluated at design speeds and speeds below that. Dynamic control of the trim is very common in high-speed vessels. But in medium-speed vessels, it is not possible to create a sufficient lift force by conventional methods. In fact, it is not economically viable to add complex appendages to the hull in exchange for the improvement that occurs in its performance. Therefore, in this study, using a small change in transom hull form, a good improvement in the dynamic behavior of the ship was observed.

Governing equations in two-phase flow are presented first and the current 6-DOF model is discussed in more depth. Subsequently, details of experimental and numerical domain setup are presented. Later, computed results are analyzed and compared against experimental measurement. Finally, the advantages of current scheme in simulation of the dynamics of high-speed craft have been presented in conclusions section.

## 2. GOVERNING EQUATIONS

### 2.1. RANS Equations

Mathematical models of fluid flow and heat transfer are generally developed according to conservation laws of physics such as conservation of mass, Newton's second law, and first law of thermodynamics (Versteeg and Malalasekera, 2007). The RANS equations, which include continuity and mass conservation equations, are the governing mathematical expressions which link pressure and velocity. The assumption of incompressible fluids has been used, which is applicable for most marine practical problems (Jasak, 1996 and Rusche, 2002).

$$\nabla U = 0 \quad (1)$$

$$\frac{\partial \rho U}{\partial t} + \nabla(\rho U U) - \nabla(\mu_{eff} \nabla U) = -\nabla p^* - gX \nabla \rho + \nabla U \nabla \mu_{eff} + \sigma \kappa \nabla \alpha \quad (2)$$

where  $\rho$  denotes the fluid density,  $U$  is the velocity vector,  $p^*$  represents the pseudo-dynamic pressure,  $g$  is the acceleration of gravity and  $X$  is the position vector. The last term on the right is the effect of surface tension,  $\sigma$  is the surface tension coefficient,  $\kappa$  is the curvature of the interface and it is calculated as follows:

$$\kappa = \nabla \frac{\nabla \alpha}{|\nabla \alpha|} \quad (3)$$

and  $\alpha$  is the indicator function, which will be commented later. Finally,  $\mu_{eff} = \rho \nu_{eff}$  is the effective dynamic viscosity, which into account the molecular dynamic viscosity plus the turbulent effects:  $\nu_{eff} = \nu + \nu_{turb}$ . Which  $\nu_{turb}$  is the turbulent kinetic viscosity and it is given by the chosen turbulence model (Rusche, 2002).

The different fluids are identified by the indicator function  $\alpha$  which is bounded between 0 and 1.  $\alpha=0$  means air phase, and  $\alpha=1$  water phase. A value of 0.5 would thus mean the cell is filled with equal volume parts of both fluids. Intensive properties of the flow like the density  $\rho$  are evaluated depending on the species variable  $\alpha$  and the value of each species  $\rho_b$  and  $\rho_f$ .

$$\rho = \alpha \rho_f + (1 - \alpha) \rho_b \quad (4)$$

The transport equation for  $\alpha$  is:

$$\frac{\partial \alpha}{\partial t} + \nabla(U \alpha) = 0 \quad (5)$$

The interface between the two fluids requires special treatment to maintain a sharp interface; numerical diffusion would otherwise mix two fluids over the whole domain (Hirt and Nichols, 1981).

### 2.2. Turbulence Modeling

The Reynolds stresses have to be modeled, when a RANS method is utilized. Most turbulence models are based on the eddy viscosity concept where the effect of the turbulence on the flow processes is described by an increased viscosity. The Reynolds stresses are then is defined by the so called Boussinesq Hypothesis which is represented equation below, where  $\kappa$  is the turbulent kinetic energy (Pope, 2001).

$$\tau_{ij} = -\rho \overline{u'_i u'_j} = \mu_t \left( \frac{\partial U_i}{\partial x_j} + \frac{\partial U_j}{\partial x_i} \right) - \frac{2}{3} \kappa \rho \delta_{ij} \quad (6)$$

$$\kappa = -\frac{1}{2} \overline{u'_i u'_j} \quad (7)$$

$$\mu_t = -\rho c_\mu L \sqrt{2\kappa} = c_\mu L V \quad (8)$$

$\mu_t$  is the turbulent viscosity and can be written as above including the constant  $c_\mu$ , the turbulent velocity  $V$  and the length scale for large-scale turbulent motion  $L$ . To calculate  $V$  and  $L$  it is necessary to express  $\kappa$  and  $\mu_t$ . The different approaches to do this divided the models into algebraic, zero-equation, one-equation and two equation models, which are all linear eddy viscosity models. Two-equation models are the most widely used models, because it is quite simple to implement these

kinds of RANS equations into a CFD program. In this work, the  $k-\epsilon$  model has been used, maybe the most used and known method in CFD simulation.

### 2.3. Body Motion Equations

The equation for the translation of the center of mass of the body is given as (Panahi *et al.* 2009):

$$m \frac{\partial V_0}{\partial t} = f \quad (9)$$

where  $m$  represents the mass of the body (ship),  $f$  is the resultant force acting on the body and  $V_0$  is the velocity vector of the center of mass. An angular momentum equation of the body is formulated in the body local coordinate system with the origin in the center of the body:

$$M \frac{d\omega}{dt} + \omega \times M\omega = n \quad (10)$$

where  $M$  is the tensor of moments of inertia,  $\omega$  is the angular velocity of rigid body, and  $n$  is the resultant moment acting on the body. The resulting force and moment acting on the ship are obtained from fluid pressure and shear force acting on the each boundary force of the body. The translations of the vessel are estimated according the computed velocity and pressure fields in the flow domain.

## 3. MATERIALS AND METHODS

### 3.1. Geometry

A wooden model with a scale of 1/15.96 was manufactured and tested in the towing tank. Also, a numerical model was designed and simulated in a Numerical Wave Tank (NWT). The geometrical and hydrostatic details of the experimental and numerical model and prototype are given in Table 1.

**Table 1 Geometric and hydrostatic characteristics of numerical and experimental model**

Main dimensions	Prototype	Model
Scale ratio	1	1/15.96
Length at water level [m]	25.548	1.60
Molded total breadth [m]	7.979	0.50
Breadth of each hull [m]	2.487	0.155
Draught [m]	1.237	0.077
Trim (aft) [mm]	109	6.8
Wetted surface area [m <sup>2</sup> ]	172.18	0.68
Displacement [Tones]	86	0.021
Design speed [ms <sup>-1</sup> ]	11.83	2.96
Block coefficient (CB) [-]	0.55	0.55
Froude number (at design speed) [-]	0.747	0.747
LCB from AP	11.40	0.71
LCF from AP	11.15	0.70

Furthermore, the front and profile view of the model and wedge geometry are given in Fig.1. In this figure, the shape of the aft of the ship is shown before the change (left) as well as the wedge added to this area (right). In various cases, the length of the wedge has been assumed fixed and its angle changed. While the length value is  $0.02L_{PP}$  and the angle varies from 4 to 10 degrees. The towing tank and numerical wave tank properties are presented in next section. The length of the stern wedge has been considered in various studies to be between 1 and 3 percent of the length of the ship (Jadmiko *et al.* 2018), (Ghadimi *et al.* 2019). In this paper, the wedge length is considered equal to 2 percent of the ship's length. The initial design of the vessel is equipped with an 8° wedge to overcome the dynamic instability. For this purpose, the experimental model was constructed in two wedge modes at 0 and 8 degrees angle. At the numerical analysis stage it was found that increasing the angle of the wedge does not necessarily lead to improved slip behavior. However, the results of the experimental analysis have been useful for the numerical solution verification under different conditions.

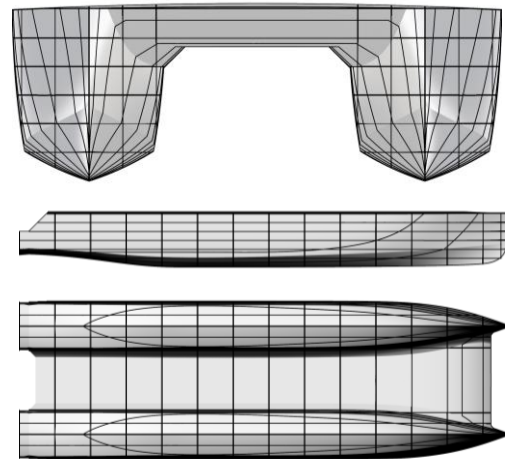


**Fig. 1. Hull lines of the model and stern profile of bare and modified stern.**

### 3.2. Experimental Setup

The towing tank has main dimensions of 400 m length, 6 m width and 4 m depth. For the current tests, the water depth was set as 3.5 m. The targeted tests are carried out in two different conditions. In the first condition, the

model is not equipped with any appendages. Based on the experiment measurements, dynamic instability was observed at high speeds. In the other condition, it is attempted to add wedge to the bottom of the model. As describe later, this equipment causes additional pressure in stern area and consequently, the unwanted trim was greatly reduced. The experimental test was performed using the 8° wedge. In the following, the effect of changing the geometry of the wedge is investigated using numerical method.

For each case, 6 different speeds are considered. During each test, the following parameters are determined:

- ✓ Trim angle
- ✓ Model sinkage
- ✓ Resistance

Figure 2 shows the towing and measurement facilities. It should be noted that the installation angle of the dynamometer with the base line has been set to 8 degrees. Figure 3 shows the process of adjusting the draft and the initial trim of the ship by adding weight to the hull. Figure 4 also shows the aft view of the body with the wedge attached to the transom.

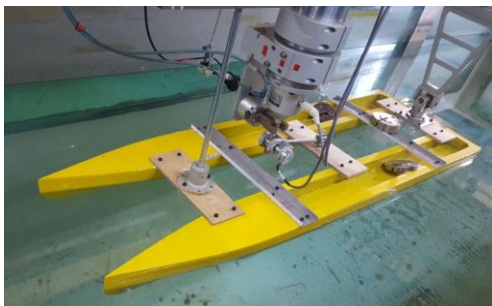


Fig. 2. Measurement devices mounted on the wooden model.



Fig. 3. Adjust the initial draft and trim using external weights.

Uncertainties in experimental analysis have been investigated according to the guidelines provided by ITTC (ITTC, 2014). Analysis of all the significant uncertainty components related to the total resistance can be summarized as:

- ✓ Hull geometry
- ✓ Dynamometer calibration
- ✓ Water temperature
- ✓ Towing speed
- ✓ Repeat tests

These standard uncertainty components will be multiplied by their sensitivity coefficients respectively and then combined to obtain the overall standard uncertainty by RSS (root-sum-squares) method.

The volume of the model designed in Rhino software is compared with the size of the wooden model. The error due to temperature changes and dynamometer calibration has also been omitted according to the documentation provided by the laboratory. Therefore, only fluctuations in the test speed during the towing test as well as changes in the amount of force and model trim due to the repetition of the test are considered. The towing test is repeated 5 times at design speed and 3 times at other speeds. The results of the uncertainty analysis of total resistance and model trim on different Froude numbers in the original hull form (wow) are presented in Table 2.



Fig. 4. Wedge made of plastic attached to the end of a wooden body.

Table 2 Summary of uncertainty analysis in resistance measurement

Fn	V [m/s]	$u'_c(R_T)$ [%]	$u'_c(Trim)$ [%]
0.137	0.46	0.98	0.45
0.274	0.92	0.96	0.45
0.412	1.38	0.86	0.44
0.569	1.84	0.88	0.44
0.686	2.30	0.82	0.42
0.749	2.53	0.79	0.41

### 3.3. Computational Model

A large 3-D domain was created in order to avoid effects from the domain boundaries to affect the flow near the hull. Due to the similarity of the solution method and the type of problem, the dimensions of the numerical domain have been selected based on the research provided by Song *et al* (2018). The computational domain is a rectangular area with dimensions of  $5.5L_{PP} \times 2.5L_{PP} \times 2.5L_{PP}$ . Due to the greater width of the study vessel in

this study than the research of Song *et al.* the length and width of the domain are slightly larger in this study. However, in some cases, larger dimensions were used, which did not significantly change the accuracy of the results.

A mesh study is performed and  $1.1 \times 10^6$  cells are selected based on the mesh independence study for forward resistance. (The grid independence test and the numerical solution uncertainty analysis are presented in Section 4.2) The vessel is enclosed by 3D rectangular computational domain over which the flow is solved. The computational domain and its dimensions are illustrated in Fig. 5 in terms of the hull length (LPP). Also, two longitudinal and transverse sections are drawn up on one of the bodies to illustrate the gridding (Fig. 6).

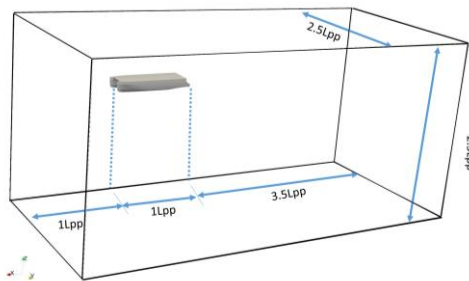


Fig. 5. Computational domain dimensions.

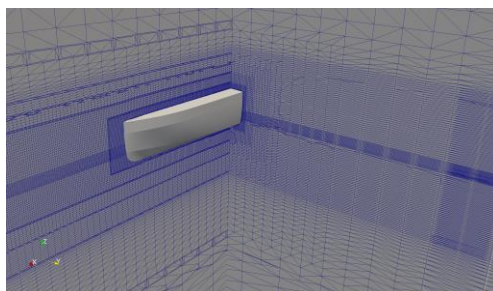
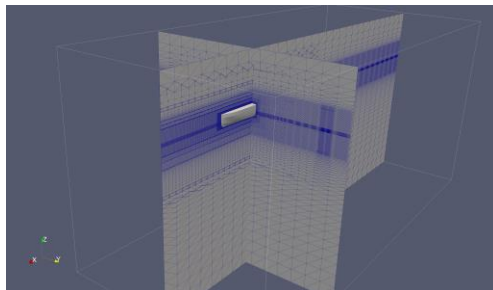


Fig. 6. Refined mesh around numerical model.

The top, side and bottom of the domain were prescribed with symmetry boundary conditions and the hull was set to wall with no slip. At the inlet, located in front of the hull, the velocity of the incident air and water was set to hull speed. The outlet located behind the hull was set to a pressure outlet. The boundary

condition details and solver parameters are presented in Table 3 and Table 4 respectively.

Table 3 Boundary conditions in numerical simulation

Boundary	Type
Inlet	Velocity inlet
Outlet	Pressure outlet
Side walls	Symmetry
Top & Bottom	Free slip
Body	No slip

Table 4 interDyMFoam solver parameters

Parameter	Setting
Solver	interDyMFoam, unsteady, two phase flow, dynamic mesh
Viscous model	$k-\epsilon$
Pressure-velocity coupling	SIMPLE
Free surface scheme	VOF
Convective acceleration discretization method	Second-order upwind
Initial time step	0.0001 [s]
Dynamic viscosity ( $\nu$ )	$1 \times 10^{-6}$ [m <sup>2</sup> /s]
Water density ( $\rho$ )	998 [kg/m <sup>3</sup> ]
Surface tension ( $\sigma$ )	0.07 [N/m]

#### 4. RESULTS AND DISCUSSION

Model sinkage and dynamic trimming are two of the most described instability characteristics in the literature. Also, total resistance is measured in different conditions. In this section, changes in the position of the center of gravity as well as the resistance force applied to it are obtained experimentally and numerically and compared with each other. Also, the effect of wedge geometry change on the hydrodynamic performance of the vessel is investigated numerically and the changes are compared with the initial model.

##### 4.1. Experimental Results

Figure 7 depicts the change of the model total resistance with the Froude number ( $Fn$ ) before and after the installation of 8° stern wedge. Froude number can be defined by:

$$Fn = \frac{V_0}{\sqrt{gL}}, \quad (11)$$

Where  $L$  is the length at water line and  $V_0$  is the model velocity. It is quite evident in this figure that in case of bare hull (wow) a significant increase in the amount of resistance has been recorded near the design speed of the ship ( $Fn=0.747$ ). The focus of this research is also on instability control and resistance reduction at this point.

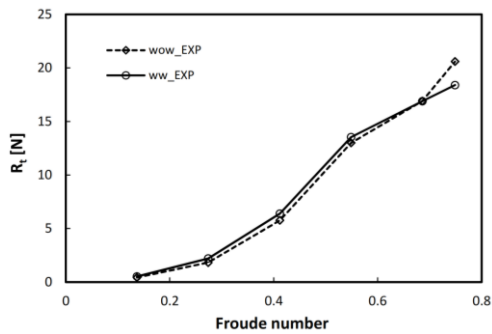


**Fig. 7. Variation of total resistance of bare model with Froude number.**

The modification of stern geometry by fitting a stern wedge is expected to reduce the resistance of the ship at medium and high speeds. As can be observed in Fig. 7, in comparison with bare hull resistance, over a certain speed range, the influence of stern wedge leads to the reduction of total resistance. The value of the model's total resistance in both bare (wow) and modified (ww) modes is 20.59 N and 18.39 N, respectively. As a result, stern wedge installation led to a 10.7% reduction in total resistance of model. It should be noted that only one wedge geometry ( $\alpha=8^\circ$ ) was used for the experimental test. The purpose of this level is to generate experimental data for numerical solution validation. Figure 8 also shows the change in resistance obtained from the experimental solution in the two initial and modified body modes. Installing the wedge at the bottom of the ship has increased its power at low speeds. The main reason is the inability of the wedge to generate lift force at such speeds. While at the Froude number of 0.7, the wedge reduces the drag force, and it has a good effect on design speed ( $Fn=0.747$ ).

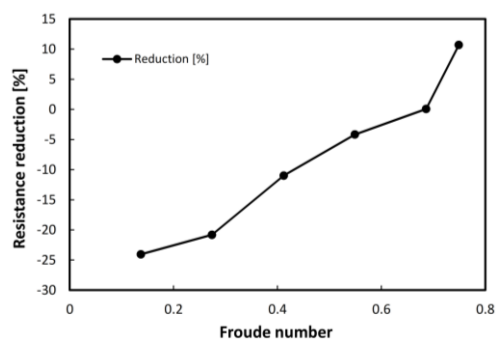


**Fig. 8. Variation of total resistance of modified model with Froude number.**

Figure 9 depicts the effect of stern wedge on the trim of the model. It is evident that installation of stern wedge presents more acceptable dynamic trimming at design speed. Also, the effect of stern wedge is more significant at high speeds. Although wedge mounting has a good effect on reducing the

dynamic trim angle, the wedge's effect on creating a proper lifting force at the ship stern area starts from  $Fn=0.5$ . While, its positive effect on resistance reduction starts from  $Fn=0.7$ . In the event that the ship's trim has fluctuated, the average fluctuation in a time interval is introduced as the dynamic trim. The positive effect of wedge mounting on trim reduction in design speed is also clearly seen.

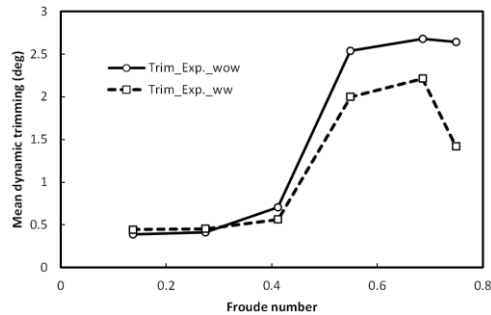


**Fig. 9. The effect of stern wedge on dynamic trimming at different Froude numbers.**

The model sinkage fluctuations at different Froude numbers are also presented in Fig. 10. In this figure, the distance from the center of mass of the ship to the baseline is shown. These changes are measured at the center of mass of the model. For this reason, changes in the location of the center of mass are largely limited. The decrease in the center of mass of the ship is due to the relative increase in the trim angle and consequently the decrease of the center of mass to in order to maintain the balance of vertical forces. As the effect of the wedge increases at higher speeds, the angle of the trim decreases, for this reason, the location of the center of mass of the vessel is also downward.

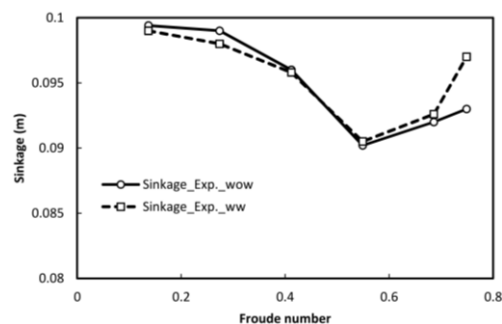
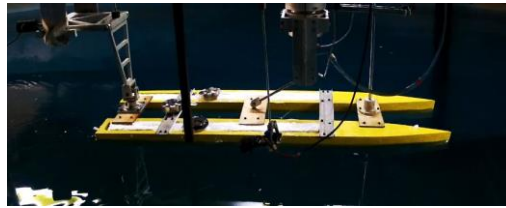


**Fig. 10. The effect of stern wedge on model sinkage at different Froude numbers.**

The model side views at different Froude numbers are presented in Fig. 11. As seen in this figure, as the Froude number increases, the value of the ship's trim will also increase. Also, the points marked by the red circles indicate a significant increase in water level due to the wave generated by the ship.



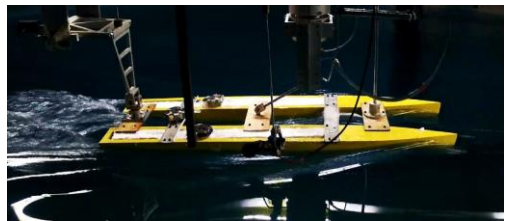
(a)  $Fn=0.137$



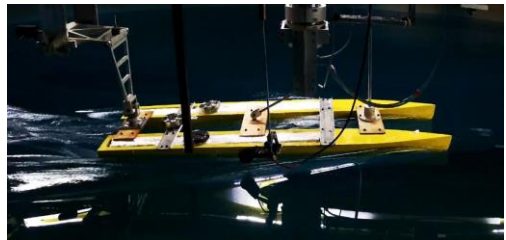
(b)  $Fn=0.274$



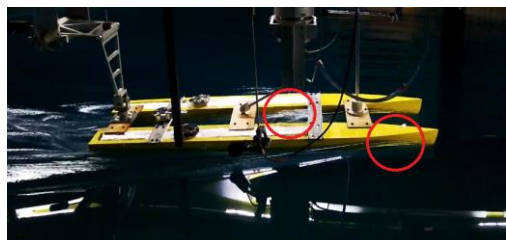
(c)  $Fn=0.412$



(d)  $Fn=0.549$



(e)  $Fn=0.686$



(f)  $Fn=0.747$

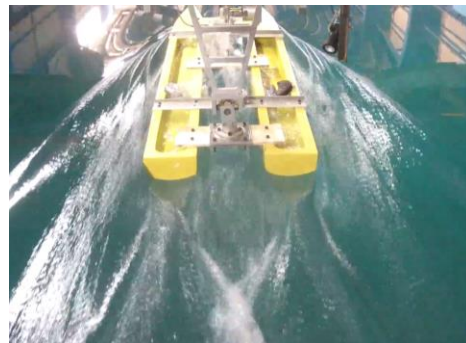
**Fig. 11. Side views of modified model at different Froude numbers.**

The waveform generated at the transom area of the bare and modified stern model is shown in Fig. 12. In this figure, the free surface is compared at design Froude number. The higher wave heights and the interaction of the

waves caused by each of the bodies in the bare model are quite evident.



(a)



(b)

**Fig. 12. Comparison of stern wave pattern in case of bare model (a) and wedge fitted model (b) at design speed.**

#### 4.2. Numerical Simulations of Bare and Modified (8° Stern Wedge) Hull

interDyMFoam solver of OpenFOAM code has been utilized to predict the resistance and dynamic characteristics of a catamaran hull form fitted with and without stern wedge. It should be noted that at this stage, the wedge is used at an angle of 8 degrees. The value of the resistance at each speed is calculated from the average of the recorded data over a suitable time interval. In Fig. 13, the drag force (resistance) oscillations are provided for an 8° wedge at  $Fn=0.747$ . Sufficient time must elapse for the results of the numerical solution to be stable. In this research, the value of the total resistance is calculated from the average of the numerical data in the last 5 seconds.

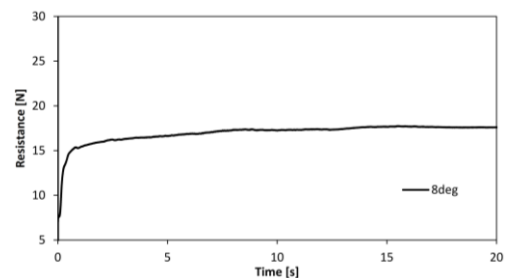


**Fig. 13. Force changes over time (8° wedge and  $Fn=0.747$ ).**

The effects of the grid on the accuracy of the results were also compared with the ship resistance in the 8 degree wedge mounting mode with the experimental values. In each case, the number of cells along the coordinate axes is increased by 5 percent. This process increases the number of cells by 20 to 30 percent. The error percentage in each case is set and finally, more than one million cells are selected for solving (Fig. 14).

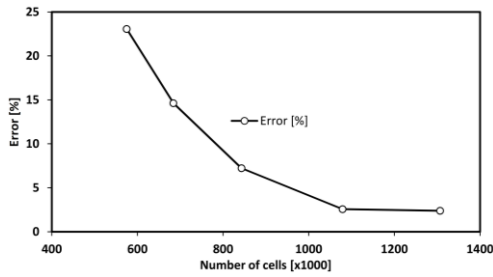


**Fig. 14. Analysis of the effect of grid selection on numerical solution accuracy.**

In this paper, the method proposed by Celik *et al.* (2008) has been used to analyze the uncertainty in numerical solution. Representative grid size has been defined as:

$$h = \left[ \frac{1}{N} \sum_{i=1}^N (\Delta V_i) \right]^{\frac{1}{3}}, \quad (12)$$

where  $\Delta V_i$  is the volume of the  $i$ th cell and  $N$  is the total number of cells used for the computations. If  $h_1 < h_2 < h_3$  and  $r_{21} = h_2/h_1$  and  $r_{32} = h_3/h_2$ , then  $p$  can be defined by:

$$p = \frac{1}{\ln(r_{21})} \left| \ln \left| \frac{\varepsilon_{32}}{\varepsilon_{21}} \right| + q(p) \right|, \quad (13)$$

$$q(p) = \ln \left( \frac{r_{21}^p - S}{r_{32}^p - S} \right),$$

$$S = 1 \cdot \text{sgn}(\varepsilon_{32}/\varepsilon_{21}),$$

where  $\varepsilon_{32} = R_3 - R_2$ ,  $\varepsilon_{21} = R_2 - R_1$ , and  $R_k$  denotes the solution on the  $k$ th grid.

Eq. (13) can be solved using an iterative method. Also, the extrapolated values are:

$$R_{ext}^{21} = (r_{21}^p R_1 - R_2) / (r_{21}^p - 1), \quad (14)$$

$$R_{ext}^{32} = (r_{32}^p R_2 - R_3) / (r_{32}^p - 1),$$

Finally, the error is estimated based on one of the following values:

Approximate relative error,

$$e_a^{21} = \left| \frac{R_1 - R_2}{R_1} \right|. \quad (15)$$

Extrapolated relative error,

$$e_{ext}^{21} = \left| \frac{R_{ext}^{12} - R_1}{R_{ext}^{12}} \right|.$$

Fine-grid convergence index,

$$GCI_{fin}^{21} = \frac{1.25 \cdot e_a^{21}}{r_{21}^p - 1}. \quad (16)$$

Finally, the uncertainty analysis obtained from Eq. (16) is presented in Table 5.

**Table 5 Calculation of discretization error in grid independency analysis procedure**

Case	N	R [N]	$GCI_{fin}$
1	575487	25.34	-
2	684597	23.60	0.69
3	842956	22.08	0.60
4	1079218	21.12	0.38
5	1306901	21.08	0.016

Therefore, it can be concluded that the uncertainty due to numerical solution in the fine-grid solution for the total resistance of the bare hull is equal to 1.6%.

The simulations were carried out for different speeds corresponding to Froude numbers up to  $Fn=0.747$  to investigate the effects of stern wedge on reduction of resistance and dynamic instability, especially at medium and high Froude numbers. The computed resistance characteristics for two numerical models of the catamaran hull with and without stern wedge have been shown in Fig. 15. The great difference between the two curves after the Froude number 0.5 is quite evident. Such a difference was also recorded in experimental analysis. It has been noted that the cause of this decrease in  $Fn=0.747$  is the effect of the wedge on the lifting force and the reduction of ship trim.

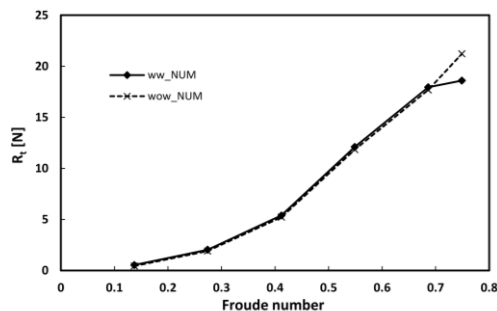


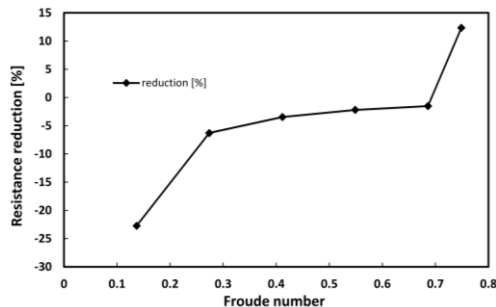
**Fig. 15. Computed total resistance of the model with 8° wedge and without wedge at different Froude numbers.**

The results suggested that the numerical analysis showed reduction in resistance for the model fitted with stern wedge at design speed.

**Table 6 Comparison of Resistance due to numerical solution and experimental analysis**

$F_n$	$V$ [m/s]	$R_{wow\_exp}$ [N]	$R_{wow\_num}$ [N]	Error <sub>wow</sub> (%)	$R_{ww\_exp}$ [N]	$R_{ww\_num}$ [N]	Error <sub>ww</sub> (%)
0.137	0.46	0.4266	0.44	3.14	0.5292	0.54	2.04
0.274	0.92	1.8226	1.91	4.80	2.2019	2.03	7.81
0.412	1.38	5.7643	5.22	9.44	6.3971	5.60	12.46
0.549	1.84	12.9941	11.84	8.88	13.5368	12.10	10.61
0.686	2.30	16.9033	17.68	4.59	16.8933	17.95	6.26
0.747	2.53	20.5940	21.22	3.04	18.3925	18.60	1.13

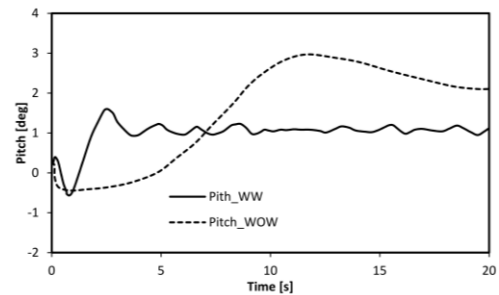
The variations in total resistance are presented in the Fig. 16 after body changes compared to the original hull. As observed in this figure, the positive effects of wedge fitting can be seen from the Froude numbers above 0.7.



**Fig. 16. Reduce or increase of total resistance compared with the bare hull condition.**

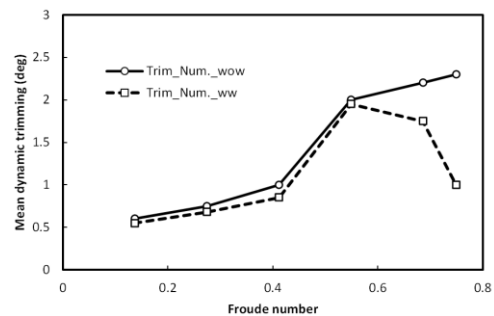
In Table 6, the ship resistances are compared in both cases with and without wedge mounting due to numerical solution and experimental analysis. In both cases with and without 8° stern wedge, the resistance values of the numerical and experimental analysis in each Froude number are compared and the error values are presented. The relative error value at low Froude numbers is slightly higher than the design speed error due to the low ship resistance value. As can be seen, in the design speed, the error due to the numerical estimation of the with-wedge vessel resistance is only 1.13%.

The use of stern wedge has had an acceptable effect on reducing power required at design speed. However, the effect of the wedge on the removal of ship dynamic instability at the design point is significant. Ship dynamic trimming changes with time at design speed is presented in Fig. 17. These results show that significant decrease in the dynamic trimming is obtained when 8° stern wedge is fitted to the bare hull. On the other hand, modified model presents more stable dynamic characteristics. The range of dynamic trim of the initial body was more than 3 degrees. While mounting the wedge, the floating trim remains at a constant degree.

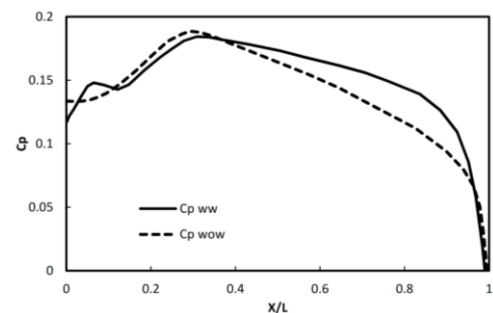


**Fig. 17. Effect of 8° stern wedge installation on model dynamic trimming at design speed.**

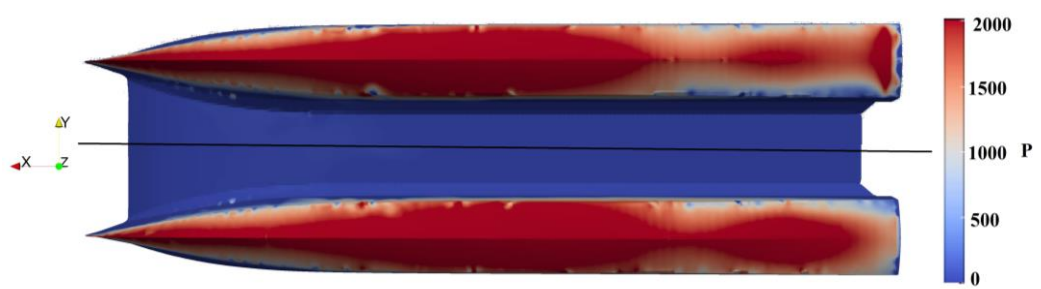
The average trim values recorded at each speed were calculated with and without the wedge. According to Fig. 18, by installing the stern wedge, there has been a significant reduction in the amount of dynamic trimming at design speed. In this case, the trimming angle has dropped by more than 50%.



**Fig. 18. Effect of stern wedge installation on numerical model trimming at different Froude numbers.**



**Fig. 19. Pressure coefficient along the bottom centerline of the ship.**



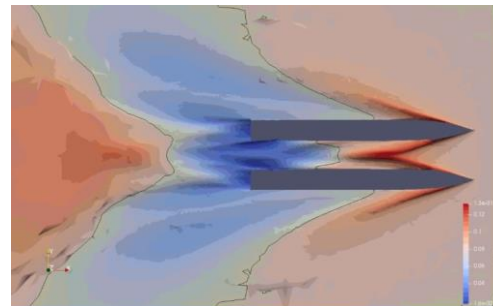
**Fig. 20. Comparison of pressure [Pa] distribution on the stern bottom zone at design speed ( $Fn=0.747$ ) for bare (down) and modified (up) hulls. ( $t=20s$ ).**

Figure 19 also, indicates the influence of using  $8^\circ$  stern wedge on the pressure coefficient of the hull at the center line of a single hull. Clearly, in case of bare hull model, the pressure coefficient indicates a gradual reduction from the mid-length to stern of the bottom. As well as, after wedge installation pressure acting at the ship stern has been increased. This increase in stern pressure leads to reduce the pressure difference between the bow and stern area, thereby reducing the unwanted dynamic trimming of the ship in calm water.

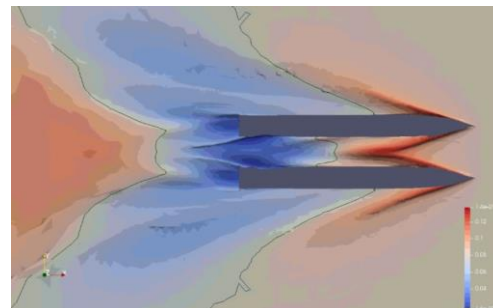
Also, the effect of  $8^\circ$  stern wedge installation on stern pressure distribution is presented in Fig. 20. As can be seen, fitting a stern wedge causes a significant increasing in pressure distribution over the stern region of the hull bottom.

Finally, iso-surface of the water-air indicator ( $\alpha$ ) is presented as free surface contour in the wake region of the transom for cases with and without fitting the stern wedge in Fig. 21. It is obvious that stern wedge serves to reduce wave heights in this region. The black line seen in this figure indicates the calm water level. The blue surfaces indicate points lower than the initial water level.

concluded that increasing the angle of the wedge to more than 6 degrees does not have a positive effect on the decrease in resistance.



(a)

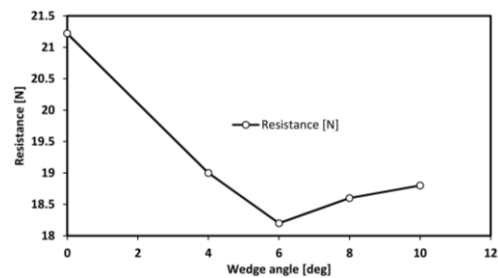


(b)

**Fig. 21. Effect of stern wedge on wave pattern near the stern region of bare (left) and wedge fitted (right) hulls.**

### 4.3. Effects of Wedge Angle Change

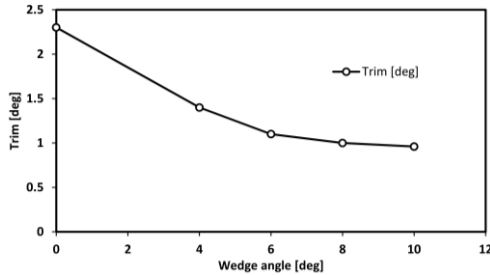
The validation process was performed on bare hull and modified hull equipped with an  $8^\circ$  wedge angle. After ensuring the accuracy of numerical solution, the effect of wedge angle on its hydrodynamic performance was investigated. Four angles of 4, 6, 8, and 10 degrees were considered for the wedge, and models fitted with each wedge were simulated. In Fig. 22, the effect of wedge geometry changes on the change in total resistance is presented at design speed ( $Fn=0.747$ ). As can be seen, the installation of the wedge in all cases has reduced the resistance of the vessel. While the wedge designed for this vessel has an 8 degree angle. An 8 degree wedge reduces ship resistance by 12%. But using a 6 degree wedge can reduce the ship's resistance up to 14% at design speed. Therefore, it can be



**Fig. 22. Effect of wedge angle on ship resistance at design speed.**

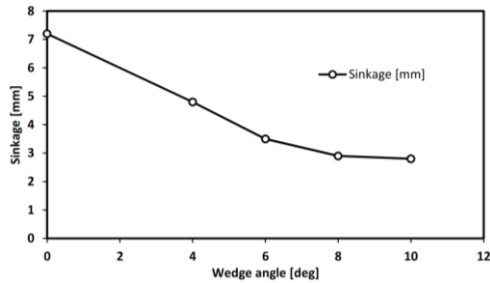
Figure 23 shows the effect of increasing the

wedge angle on the dynamic trimming of the ship. As evident in this figure, increasing the wedge angle causes an increase in hydrodynamic lift at the end of the hull bottom and as a result, ship trim decreases. However, slope of the resultant curve decreases with an increase in the wedge angle.



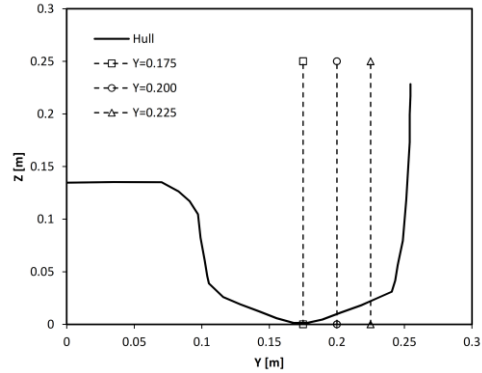
**Fig. 23. Effect of wedge angle on dynamic trimming at design speed.**

Figure 24 also shows the effect of changing the wedge angle on the location of the COG relative to its original location. These changes are measured relative to the state where the ship's speed is zero. The general trend of vertical changes of the ship's COG is perfectly in line with the fluctuations of the trim. Of course, as the wedge angle increases further, its effect on reducing the height of the center of mass also decreases.

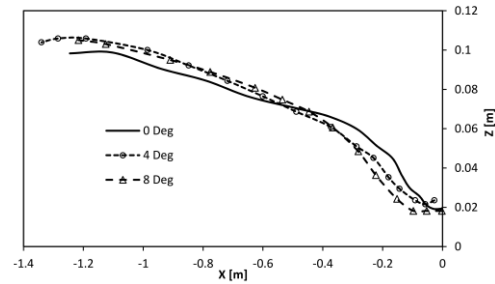


**Fig. 24. Effect of wedge angle on sinkage at design speed.**

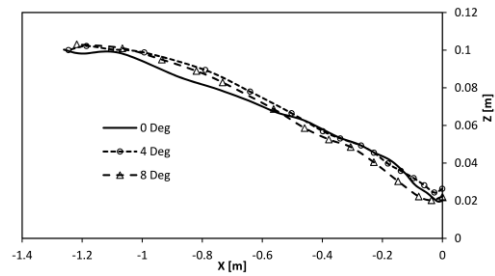
Finally, the elevations of the free surface along three different longitudinal sections are compared at different wedge angles. The exact position of these sections is depicted in Fig. 25. Also, the effect of the wedge installation on the free surface of the fluid is quite obvious in Fig. 26. Exactly in the centerline of the half-body ( $y=0.175m$ ). In case of wedge installed vessel, a free surface through is observed near the ship transom. Also, the elevation recorded for the free surface adjacent to the transom, depends entirely on the trim and sinkage of the ship. The minimum height of the free surface depends on the angle of the wedge. However, wedge installation has eliminated short-range oscillations of the water surface. This trend is observed in the other two sections. But, the effect of wedge angle on the water level fluctuations is less in these sections.



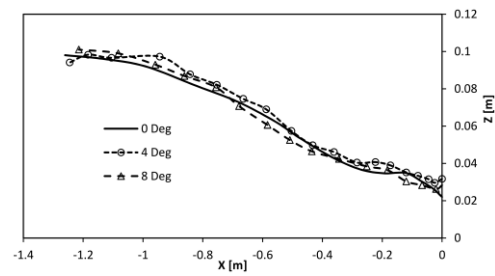
**Fig. 25. Position of longitudinal sections of free surface measurement.**



(a)  $y=0.175m$



(b)  $y=0.200m$



(c)  $y=0.225m$

**Fig. 26. Free surface elevation at different longitudinal sections at design speed.**

## 5. CONCLUSIONS

Numerical and experimental investigation have been performed, based on the scaled model test and 6-DOF CFD simulations, for validation of proposed model of semi-displacement catamaran hull under medium and high-speed conditions. Finite Volume Method (FVM) and Volume of Fluid (VOF)

scheme have been implemented to simulate the free surface incompressible problem. interDyMFoam solver of OpenFOAM open source code has been utilized to consider the effects of ship motions based on dynamic mesh technique. In addition, a wooden model with a scale of 15.96 was made and evaluated under different conditions with and without stern wedge were considered. Comprehensive study of the effects of two different conditions on ship dynamic characteristics has been performed. The reported results indicate the without wedge model was subjected to dynamic instability at high speeds. The main objective of this study is to predict forward resistance and dynamic instability reduction of a semi-displacement twin hull vessel when fitted with stern wedge. Based on numerical simulations and experimental measurements, following conclusions can be reached:

- ✓ The use of stern wedges has had a good effect on reducing dynamic instability as well as vessel resistance at design speed. In the case of this particular vessel, this is one of the simplest methods of dynamic control of the ship.
- ✓ Based on research in the field of high-speed crafts, the angle of 8 degrees was considered as an initial value for the wedge. But with further examination of the other angles, it was found that the effectiveness of the 6-degree angle is slightly higher. At this angle, the greatest reduction in total resistance is observed at design speed (More than 14 percent).
- ✓ When stern wedge is fitted, the model dynamic trimming is reduced by 50% at design speed.
- ✓ In comparison with bare hull, the total drag force due to fitting stern wedge is reduced by 14.2%. However, the initial design of the vessel was based on an 8 degree angle wedge. At this angle, the amount of resistance reduction is 2 percent lower than the angle of 6 degrees.
- ✓ The study clearly state that the reduction in total resistance starts in comparison with bare hull resistance at Froude numbers between  $0.7 < Fn < 0.747$ .
- ✓ The large area of high pressure generated by installation of the stern wedge resulted in creation of a greater lift force near the stern area and lead to optimizing the unwanted dynamic trimming of the ship in calm water.
- ✓ Installation of the wedge reduces small fluctuations in water level behind the ship. As the amplitude of the generated wave increases.

Based on the acquired results, it is concluded that installation of stern wedge has the great effect on resistance reduction of this hull form.

The unwanted trim clearly increases when the stern wedge was installed. Decreasing this trim leads to lower total resistance at medium and high velocities.

The aim of the present study has been to present a numerical method for accurately predict ship dynamic instabilities, especially at high speeds. In conclusion, it is also found that the proposed numerical method using RANS formulation for the incompressible field and the VOF scheme and dynamic mesh model are appropriate for simulation of ship dynamics at high speeds.

#### ACKNOWLEDGEMENTS

The authors would like to express their deep and sincere gratitude to “National Persian Gulf Towing Tank” for giving the opportunity to do research and providing invaluable guidance throughout this research.

#### REFERENCES

- Avci, A. G. and B. Barlas (2019). An experimental investigation of interceptors for a high speed hull. *International Journal of Naval Architecture and Ocean Engineering* 11(1), 256-273.
- Bojovic, P., P. K. Sahoo and M. Salas (2004). A Study on Stern Wedges and Advanced Spray Rail System on Calm Water Resistance of High-Speed Displacement Hull Forms. *Proc. of International Maritime Conference, Pacific, Sydney, Australia*.
- Celik, I., U. Ghia, P. J. Roache, C. Freitas, C. Coloman, P. E. Raad (2008) Procedure for Estimation and Reporting of Uncertainty Due to Discretization in CFD Applications, *Journal of Fluids Engineering* 130(7): 078001.
- Cumming, D, R. Pallard, E. Thornhill, D. Hally and M. Dervin (2006) Hydrodynamic Design of a Stern Flap Appendage for the HALIFAX Class Frigates, *MARI-TECH*, Halifax, Canada, 1–14.
- Day, A. H. and Ch. Cooper (2011). An experimental study of interceptors for drag reduction on high-performance sailing yachts. *Ocean Engineering* 38, 983-994.
- Ghadimi, P, S. M. Sajedi and S. Tavakoli (2019). Experimental Study of the Wedge Effects on the Performance of a Hard-chine Planing Craft in Calm Water. *Scientia Iranica* 26(3), 1316-1334.
- Hirt, C. W. and B. D. Nichols (1981). Volume of fluid (VOF) method for the dynamics of free boundaries. *Journal of computational physics* 39, 201–225.

- ITTC (2014), Recommended Procedures. General Guideline for Uncertainty Analysis in Resistance Tests. 7.5-02-02-02.
- Jadmiko, E., I. Syarif and L. Arif (2018). Comparison of Stern Wedge and Stern Flap on Fast Monohull Vessel Resistance. *International Journal of Marine Engineering Innovation and Research* 3(2), 41-49.
- Jang, H. S., J. Lee, Y. Joo, J. J. Kim and H. H. Chun (2009), Some practical design aspects of appendages for passenger vessels, *International Journal of Naval Architecture and Ocean Engineering* 1(1), 50-56.
- Jangam, S., V. A. Subramanian and P. Krishnankutty (2019). Computational Study on the Hydrodynamic Effects of Interceptors Fitted to Transom of Planing Vessel. *Proceedings of the Fourth International Conference in Ocean Engineering (ICOE2018)*, Lecture Notes in Civil Engineering 22, Singapore.
- Jasak, H. (1996), Error Analysis and Estimation for the Finite Volume Method with Applications to Fluid Flows, Imperial College, London, UK (Ph. D. thesis).
- Jensen, N. and R. Latorre (1992). Prediction of influence of stern wedges on power boat performance. *Ocean Engineering* 19(3), 303-312.
- John, Sh., M. D. K. Khan, P. C. Praveen, M. Korulla and P. K. Panigrahi (2011). Hydrodynamic performance enhancement using stern wedges, stern flaps and interceptors for ships. *Conference: ICSOT, INDIA*.
- Karafiath, G. and S. C. Fisher (1987). The effect of stern wedges on ship powering performance. *Naval Engineering Journal* 99(3), 27-38.
- Karimi, H. M., M. S. Seif and M. Abbaspoor (2013). An experimental study of interceptor's effectiveness on hydrodynamic performance of high-speed planing crafts. *Polish maritime research* 2(78), 21-29.
- Mansoori, M. and A. C. Fernandes (2015). Hydrodynamics of the interceptor on a 2-D flat plate by CFD and experiments. *Journal of Hydrodynamics* 27(6), 919-933.
- Mansoori, M. and A. C. Fernandes (2016). The interceptor hydrodynamic analysis for controlling the porpoising instability in high speed. *Applied Ocean Research* 57, 40-51.
- Mansoori, M., A. C. Fernandes and H. Ghassemi (2017). Interceptor design for optimum trim control and minimum resistance of planing boats. *Applied Ocean Research* 69, 100-115.
- Panahi, R., E. Jahanbakhsh and M. S. Seif (2009). Towards simulation of 3D nonlinear high-speed vessels motion. *Ocean Engineering* 36, 256-265.
- Park, J. Y., H. Choi, J. Lee, H. Choi, J. Woo, S. Kim, D. J. Kim, S. Y. Kim and N. Kim (2019). An experimental study on vertical motion control of a high-speed planing vessel using a controllable interceptor in waves. *Ocean Engineering* 173, 841-850.
- Pope, S. B. (2001). *Turbulent Flows*. Cambridge University Press, Cambridge.
- Rusche, H. (2002), *Computational Fluid Dynamics of Dispersed Two-phase Flows at High Phase Fractions*, Imperial College, London, UK (Ph.D.thesis).
- Sajedi, S. M., P. Ghadimi, M. Sheikholeslami and M. A. Ghassemi (2019). Experimental and numerical analyses of wedge effects on the rooster tail and porpoising phenomenon of a high-speed planing craft in calm water. *Proceedings of the Institution of Mechanical Engineers, Part C: Journal of Mechanical Engineering Science*.
- Salas, M. and G. Tampier (2013). Assessment of appendage effect on forward resistance reduction. *Ship Science & Technology* 7(13), 37-45.
- Song, K., Ch. Guo, Ch. Wang, J. Gong and P. Li (2019). Investigation of the influence of an interceptor on the inlet velocity distribution of a waterjet-propelled ship using SPIV technology and RANS simulation. *Ships and Offshore Structures*.
- Song, K., Ch. Guo, J. Gong, P. Li and L. Wang (2018). Influence of interceptors, stern flaps, and their combinations on the hydrodynamic performance of a deep-vee ship. *Ocean Engineering* 170, 306-320.
- Versteeg, H. K. and W. Malalasekera (2007). *An Introduction to Computational Fluid Dynamics: The Finite Volume Method*. Longman Scientific & Technical, New York.